

# SAR Signal Reconstruction from Non-Uniform Displaced Phase Centre Sampling

Gerhard Krieger, Nicolas Gebert, Alberto Moreira  
 Microwaves and Radar Institute, DLR, Oberpfaffenhofen, Germany  
 E-Mail: Gerhard.Krieger@dlr.de

**Abstract** -The displaced phase centre (DPC) technique will enable a wide swath SAR with high azimuth resolution. In a classic DPC system, the PRF has to be chosen such that the SAR carrier moves just one half of its antenna length between subsequent radar pulses. Any deviation from this PRF will result in a non-uniform sampling of the synthetic aperture. This paper shows that an unambiguous reconstruction of the SAR signal is also possible in case of such a non-optimum PRF. For this, an innovative reconstruction algorithm is derived, which enables a recovery of the unambiguous Doppler spectrum also in case of a non-uniform sampling of the synthetic aperture. This algorithm will also have a great potential for multistatic satellite constellations as well as the dual receive antennas in Radarsat II and TerraSAR-X.

## I. INTRODUCTION

Wide swath imaging and high azimuth resolution pose contradicting requirements on SAR system design. To overcome this fundamental limitation, several innovative techniques have been suggested which use multiple apertures to acquire additional samples along the synthetic aperture. The apertures may be either on a single platform like in the classical Displaced Phase Centre (DPC) technique [1]-[6] or on different platforms [7]-[10] leading to a multistatic SAR where the size of each individual receiver is reduced. Fig. 1 shows one example for each scenario, where a single transmitter illuminates a wide swath and  $n$  sub-apertures record simultaneously the scattered signal from the illuminated footprint. Under ideal conditions, this will allow for a reduction of the PRF by a factor of  $n$  without rising azimuth ambiguities [1][10]. For optimum performance, the along-track displacement of the sub-apertures  $i=\{2,\dots,n\}$  relative to the first receiver ( $i=1$ ) should be chosen as

$$x_i - x_1 \approx \frac{2v}{PRF} \left( \frac{i-1}{n} + k_i \right) \quad k_i \in Z \quad (1)$$

which will result in a uniform sampling of the received SAR signal. In this equation,  $PRF$  is the pulse repetition frequency of the transmitter and  $v$  is the velocity of the SAR carrier. In a single platform system, all  $k_i$  will be zero. Since the sub-aperture distance and the platform velocity are fixed in this case, a specific  $PRF$  will be required:

$$PRF = \frac{2 \cdot v}{n \cdot \Delta x} \quad (2)$$

where we assume an antenna with  $n$  sub-aperture elements separated by  $\Delta x = x_{i+1} - x_i$ . The  $PRF$  in a single-platform DPC system has thus to be chosen such that the SAR platform

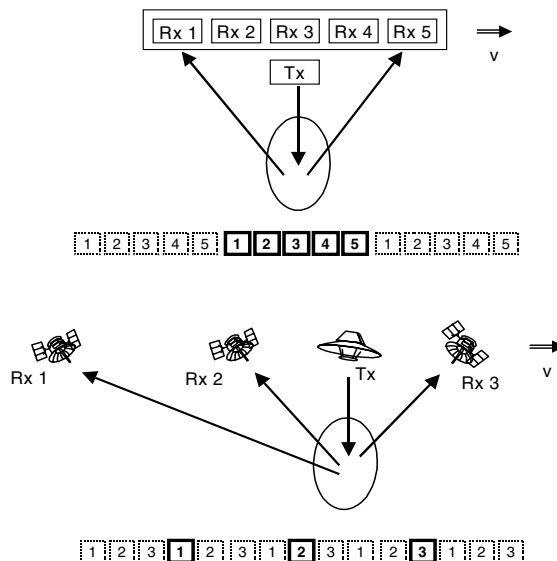


Fig. 1: Multiple aperture sampling for a single platform system (top) and a distributed satellite array (bottom). The effective phase centres are shown as squares. Solid squares correspond to samples of the synthetic aperture for the illustrated transmitter (Tx) and receiver (Rx) positions. Dotted squares are for previous and subsequent transmit pulses assuming an appropriate PRF.

moves just one half of the total antenna length between subsequent radar pulses. However, such a rigid selection of the PRF may be in conflict with the timing diagram for some incident angles. It will furthermore exclude the opportunity to use an increased PRF for improved azimuth ambiguity suppression.

## II. RECONSTRUCTION FROM NON-UNIFORM PRF

In the following, an innovative reconstruction algorithm will be derived which allows for an unambiguous recovery of the Doppler spectrum in case of a non-uniform sampling of the SAR signal. The only requirement is that the samples do not coincide. Such an algorithm has a great potential for any multi-aperture system, be it multistatic with sparsely distributed receiver satellites or be it a classic DPCA system like Radarsat II [5] or TerraSAR-X [6]. The data acquisition in a multiple aperture SAR can be considered as a linear system with multiple receiver channels, each described by a linear filter  $h_i(t)$  with transfer function  $H_i(f)$  (cf. Fig. 2). For such a system there exist a lot of powerful theorems in linear systems theory. Of special importance for the present context is a generalization of the sampling theorem according to which a

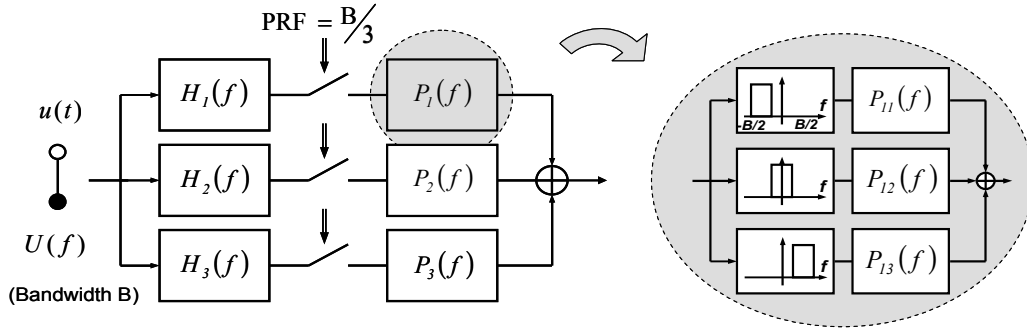


Fig. 2: Left: Reconstruction for multi-channel subsampling in case of three channels. Right: Each reconstruction filter  $P_i$  consists of  $n$  bandpass filters  $P_{ij}$ .

band-limited signal  $u(t)$  is uniquely determined in terms of the samples  $h_i(nT)$  of the responses  $h_i(t)$  of  $n$  linear systems with input  $u(t)$  sampled at  $1/n$  of the Nyquist frequency [11]. In order to be valid, the transfer functions of the linear filters may be selected in a quite general sense, but not arbitrarily (for details, see [11]). A block diagram for the reconstruction from the subsampled signals is shown in Fig. 2. The reconstruction consists essentially of  $n$  linear filters  $P_i(f)$  which are individually applied to the subsampled signals of the receiver channels and then superimposed. Each of the reconstruction filters  $P_i(f)$  can again be regarded as a composition of  $n$  bandpass filters  $P_{ij}(f)$ , where  $1 \leq j \leq n$ . As shown in [11], the reconstruction filters can be derived from a matrix  $\mathbf{H}(\mathbf{f})$  consisting of the  $n$  transfer functions  $H_i(f)$  which have to be shifted by integer multiples of the PRF in the frequency domain:

$$\mathbf{H}(\mathbf{f}) = \begin{bmatrix} H_1(f) & \dots & H_n(f) \\ H_1(f + PRF) & \dots & H_n(f + PRF) \\ \vdots & \ddots & \vdots \\ H_1(f + (n-1) \cdot PRF) & \dots & H_n(f + (n-1) \cdot PRF) \end{bmatrix} \quad (3)$$

The reconstruction filters  $P_{ij}(f)$  are then derived from an inversion of the matrix  $\mathbf{H}(\mathbf{f})$  as:

$$\mathbf{H}^{-1}(\mathbf{f}) = \begin{bmatrix} P_{11}(f) & P_{12}(f + PRF) & \dots & P_{1n}(f + (n-1)PRF) \\ P_{21}(f) & P_{22}(f + PRF) & \dots & P_{2n}(f + (n-1)PRF) \\ \vdots & \vdots & \ddots & \vdots \\ P_{n1}(f) & P_{n2}(f + PRF) & \dots & P_{nn}(f + (n-1)PRF) \end{bmatrix} \quad (4)$$

### III. ANALYTIC EXAMPLE

As a simple example we consider a bistatic SAR with two receiver channels having the same azimuth antenna pattern. This two-channel system may serve as an example for the unambiguous recovery of the Doppler spectrum resulting from a SAR signal recorded by the split antenna technique in TerraSAR-X and Radarsat II. As shown in more detail in [10], the following expressions for  $\mathbf{H}(\mathbf{f})$  and the reconstruction filters  $P_i(f)$  are obtained:

$$\mathbf{H}(\mathbf{f}) = \begin{bmatrix} \exp\left[-j\pi\left(\frac{\Delta x_1^2}{2\lambda r_0} + \frac{\Delta x_1}{v}f\right)\right] & \exp\left[-j\pi\left(\frac{\Delta x_2^2}{2\lambda r_0} + \frac{\Delta x_2}{v}f\right)\right] \\ \exp\left[-j\pi\left(\frac{\Delta x_1^2}{2\lambda r_0} + \frac{\Delta x_1}{v}(f + PRF)\right)\right] & \exp\left[-j\pi\left(\frac{\Delta x_2^2}{2\lambda r_0} + \frac{\Delta x_2}{v}(f + PRF)\right)\right] \end{bmatrix} \quad (5)$$

$$P_1(f) = \begin{cases} \frac{\exp(j\pi\Delta x_1^2/2\lambda r_0) \cdot \exp(j\pi\Delta x_1 f/v)}{1 - \exp[j\pi \cdot PRF \cdot (\Delta x_2 - \Delta x_1)/v]} & -PRF < f < 0 \\ \frac{\exp(j\pi\Delta x_1^2/2\lambda r_0) \cdot \exp(j\pi\Delta x_1 f/v)}{1 - \exp[j\pi \cdot PRF \cdot (\Delta x_1 - \Delta x_2)/v]} & 0 < f < PRF \end{cases} \quad (6)$$

$$P_2(f) = \begin{cases} \frac{\exp(j\pi\Delta x_2^2/2\lambda r_0) \cdot \exp(j\pi\Delta x_2 f/v)}{1 - \exp[j\pi \cdot PRF \cdot (\Delta x_1 - \Delta x_2)/v]} & -PRF < f < 0 \\ \frac{\exp(j\pi\Delta x_2^2/2\lambda r_0) \cdot \exp(j\pi\Delta x_2 f/v)}{1 - \exp[j\pi \cdot PRF \cdot (\Delta x_2 - \Delta x_1)/v]} & 0 < f < PRF \end{cases} \quad (7)$$

The numerator of the reconstruction filters  $P_i(f)$  can be regarded as compensating the different time delays and phase shifts within each branch, while the conjugate mirror structure in the denominator is responsible for a cancellation of the ambiguous frequencies within each branch. It becomes also clear that the denominator will vanish for equal receiver positions ( $\Delta x_2 = \Delta x_1$ ) and a reconstruction becomes impossible due to the coinciding samples in azimuth.

### IV. RANGE CELL MIGRATION

Up to now we have only considered the unambiguous reconstruction of the azimuth SAR signal. In a next step, we will hence discuss the effects of range cell migration and their implications on 2D signal reconstruction. Each receiver in a multistatic SAR will have its own range history. As a consequence, the range cell migration may show a relative offset and a difference in range curvature (cf. Fig. 3).

As an example to evaluate these effects, we consider one single and one multi-platform system with a slant range  $r_0 = 700$  km and an azimuth resolution of 1 m. The single platform system is a symmetric configuration (Fig. 1, top) with a maximum Rx aperture separation of 10 m. The evaluated multi-platform system consists of three passive receivers following the active transmitter with a separation of 250 m

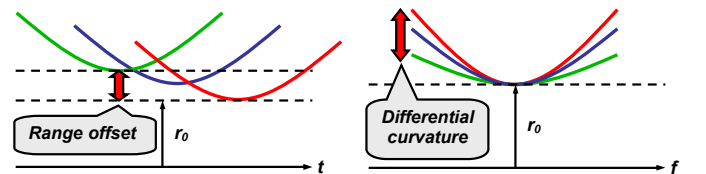


Fig. 3: Relative range offset (left) and differential range curvature (right) in a multistatic SAR system.

between each satellite. As can be seen from the upper part of Table 1, the differential range curvature can be neglected for both configurations and frequency bands, while for a multistatic system with large receiver spacing the relative range offset might require a relative range shift to correct for.

TABLE 1: RANGE MIGRATION AND RECONSTRUCTION FILTER MISMATCH.

	Single-platform	Multi-platform
Max. receiver spacing	10 m	500 m
Relative range offset	$< 10^{-5}$ m	$< 0.1$ m
Differential range curvature	$< 10^{-9}$ m (X-Band) $< 10^{-7}$ m (L-Band)	$< 10^{-4}$ m (X-Band) $< 10^{-3}$ m (L-Band)
$\Delta\phi$ (in deg)	$< 10^{-3}$ (X-Band)	$< 11$ (X-Band)
(uncompressed, $\tau = 10\mu\text{s}$ )	$< 10^{-4}$ (L-Band)	$< 2$ (L-Band)
$\Delta\phi$ (in deg)	$< 10^{-5}$ (X-Band)	$< 0.1$ (X-Band)
(range compressed)	$< 10^{-4}$ (L-Band)	$< 0.6$ (L-Band)

The consequences on the SAR focusing depend on the chosen processing scheme. Basically, a brute force approach is possible, where the complete data are reconstructed for every range  $r_0$ . As this could lead to unacceptably long processing times, the simple processing scheme shown in Fig. 4 is proposed, where the unambiguous SAR signal is recovered prior to a conventional 2-D SAR focusing including the correction for range cell migration. According to this scheme, the unambiguous azimuth signal is reconstructed independently for each range bin by adapting the filters  $P_i$  not to the range of a corresponding point target but to the actual range in the recorded raw data array. This will cause a mismatch between the point target response and the reconstruction filter. As can be seen from Eqs. 6 and 7, the dependency of  $P_i$  on  $r_0$  is described by  $\exp(j\pi\Delta x_i^2/2\lambda r_0)$ , which determines the phase error occurring due to the fact that the response of a target at  $r_0$  is spread over range and therefore partly reconstructed with filters adapted to adjacent slant ranges  $r_0 + \Delta r$ . The expected maximum phase mismatch is shown in the lower part of Table 1. The results show, that this error can be neglected for range compressed data but has to be taken into account during the reconstruction of uncompressed data when the receiver spacing becomes too large.

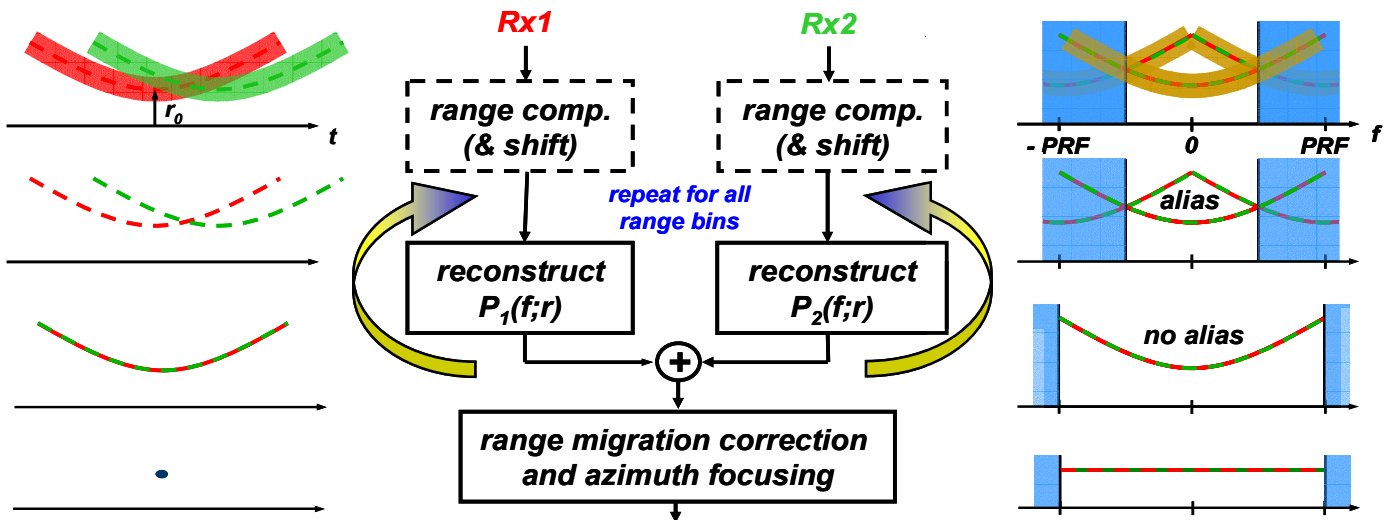


Fig. 4: Fast 2-D reconstruction algorithm. Range compression prior to the ambiguity reconstruction is mandatory only when the receiver spacing becomes too large.

## V. SIMULATION RESULTS

First simulation results of the suggested reconstruction algorithm in case of a multistatic satellite array with three receivers have been presented in [12]. Here, we will show some simulation results for the dual receive antenna in TerraSAR-X. The relevant system parameters are summarised in Table 2.

TABLE 2: PARAMETERS FOR DUAL RECEIVE ANTENNA.

Wavelength	3.1 cm
PRF	3600 Hz
Velocity	7600 m/s
Antenna Length (Tx)	2.4 m (4.8 m / 2)
Number of Subapertures (Rx)	2
Sub-Aperture Length (Rx)	2.4 m (4.8 m / 2)
Slant Range	700 km
Channel SNR	20 dB

Fig. 5 shows the results for a reconstruction from non-uniform DPCA sampling. For better illustration, an extended scatterer has been chosen in this simulation. Furthermore, independent white noise has been added to each sub-aperture signal to account for differences in the two receiver channels. It becomes clear that the signal from each channel is strongly ambiguous (left) while the coherent reconstruction of the two sub-sampled SAR signals will provide an efficient ambiguity suppression (right). The algorithm has also been tested with real SAR data acquired by the DLR E-SAR system. Since there is currently no displaced phase centre mode in the E-SAR system, monostatic data were used in this example. The data, which have an original sampling frequency  $f_s$ , were filtered with an ideal low pass of bandwidth  $B=f_s/10$  to get SAR data  $u(t)$  over-sampled by a factor of 10. Then, the ambiguous inputs to the two DPCA channels have been formed by taking every  $20^{\text{th}}$  sample for each channel. Selecting adjacent samples for the two channels will result in a maximum non-uniform sampling while a distance of 10 samples will yield a uniform sampling. After filtering with  $P_j$  and coherent summation, the monostatic SAR processing

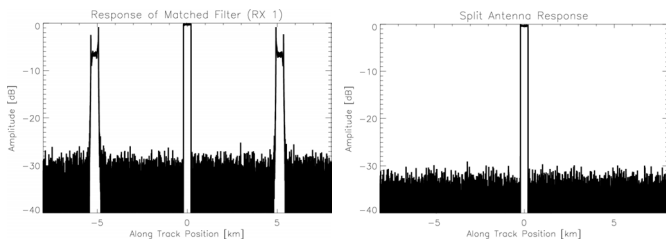


Fig. 5: Azimuth response for one sub-aperture (left) and after non-uniform DPCA reconstruction (right).

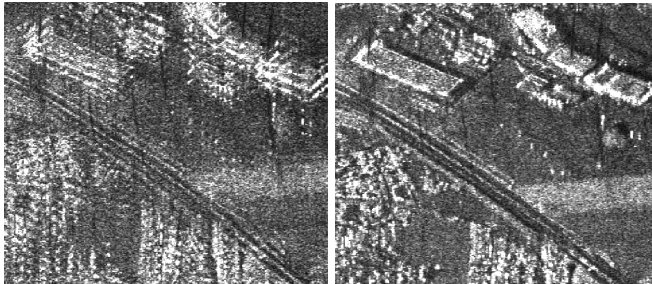


Fig. 6: Ambiguous image for one channel (left) and reconstruction after non-uniform DPCA sampling (right).

follows. Fig. 6 compares the reconstruction result for a maximum non-uniform sampling with the SAR image of one ambiguous channel. It is clear, that the ambiguities are well-suppressed in the image resulting from the non-uniform DPCA reconstruction.

Further simulations have been carried out to verify the correct reconstruction with the processing scheme shown in Fig. 4. For this, we assume a system with radar parameters specified in Table 2. The transmitted chirp has a bandwidth of 110 MHz with pulse duration of 10  $\mu$ s and the reconstruction was applied to the uncompressed raw data. Fig. 7 compares the reconstructed impulse responses for the monostatic case (top) to the TerraSAR-X case with an Rx aperture spacing of 2.4m (middle) and a sparse array configuration with a receiver spacing of 500m (bottom). All simulations show a good reconstruction of the point target.

## VI. CONCLUSIONS

An innovative algorithm for the suppression of azimuth ambiguities in case of non-uniform DPCA sampling has been derived. This reconstruction algorithm can be regarded as a time-variant digital beamforming on receive, which combines the individual receiver signals in a linear space-time processing. The algorithm is directly applicable to systems relying on the displaced phase centre (DPC) technique, like the Quad Array [2] and HRWS [3] SAR or the dual receive antenna approaches in TerraSAR-X [6] and Radarsat II [5], thereby avoiding any stringent PRF restriction. The algorithm will also be useful for ambiguity suppression in a distributed SAR with multiple receiver satellites. However, any cross-track separation of the receivers will introduce an additional phase in the received signals, which has to be compensated, e.g., via the simultaneous acquisition of a digital elevation model in case of multiple

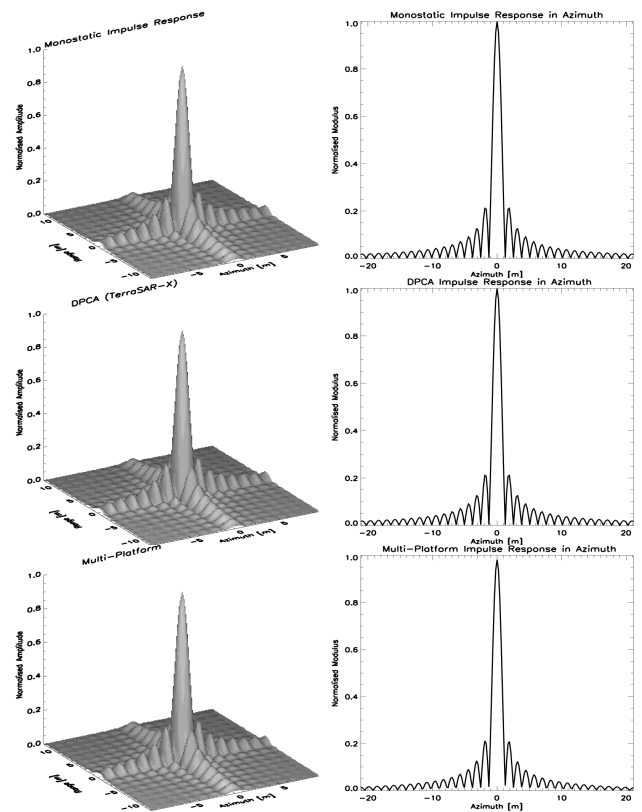


Fig. 7: Impulse response (left) and azimuth slice (right) for monostatic (top), DPCA (middle) and sparse array reconstruction (bottom).

satellites. The processing of these data will then lead to a nonlinear combination of cross-track interferometry and digital beamforming on receive.

## REFERENCES

- [1] A. Currie and M.A. Brown, Wide-Swath SAR, IEE Proceedings - Radar Sonar and Navigation 139 (2), pp 122-135, 1992
- [2] G.D. Callaghan and I.D. Longstaff, Wide Swath Spaceborne SAR Using a Quad Element Array, IEE Radar Sonar and Navigation 146(3), pp 159-165, 1999
- [3] M. Suess, B. Grafmüller, R. Zahn, A Novel High Resolution, Wide Swath SAR System, IGARSS 2001
- [4] M. Younis, C. Fischer, W. Wiesbeck, Digital Beamforming in SAR systems, IEEE Trans. Geosci. Remote Sensing 41 (7), pp. 1735-1739, 2003
- [5] L. Brule, H. Baeggli, Radarsat-2 Program Update, IGARSS 2002.
- [6] J. Mittermayer, H. Runge, Conceptual Studies for Exploiting the TerraSAR-X Dual Receiving Antenna, IGARSS 2003.
- [7] N.A. Goodman, S.C. Lin, D. Rajakrishna, J.M. Stiles, Processing of Multiple-Receiver Spaceborne Arrays for Wide Area SAR, IEEE Trans. Geosci. Remote Sensing 40 (4), pp 841-852, 2002.
- [8] G. Krieger and A. Moreira, Potentials of Digital Beamforming in Bi- and Multistatic SAR, IGARSS 2003.
- [9] J.P. Aguttes, "The SAR Train Concept: Required Antenna Area Distributed over N Smaller Satellites, Increase of performance by N", IGARSS 2003.
- [10] G. Krieger, N. Gebert, A. Moreira, Unambiguous SAR Signal Reconstruction from Non-Uniform Displaced Phase Centre Sampling, to appear in IEEE Geoscience and Remote Sensing Letters (see also EUSAR 2004).
- [11] J.L. Brown, Multi-Channel Sampling of Low-Pass Signals, IEEE Transactions on Circuits and Systems 28 (2), pp.101-106, 1981
- [12] G. Krieger, H. Fiedler, M. Rodriguez, D. Hounam, A. Moreira, System Concepts for Bi- and Multistatic SAR Missions, Proc. International Radar Symposium, Dresden, Germany, pp. 331-339, 2003 (see also Proc. of ASAR Workshop June 2003).